SUPPLEMENTARY MATERIAL OF THE ARTICLE
Intrinsic Fluid Interfaces and Non-Locality

Eva M. Fernández
Departamento de Física Fundamental, Universidad Nacional de Educación a Distancia, 28080, Madrid, Spain
Instituto de Ciencia de Materiales de Madrid, CSIC, 28049, Madrid, Spain

Enrique Chacón
Instituto de Ciencia de Materiales de Madrid, CSIC, 28049, Madrid, Spain and
Instituto de Ciencia de Materiales Nicolás Cabrera,
Universidad Autónoma de Madrid, Madrid, 28049, Spain

Pedro Tarazona
Departamento de Física Teórica de la Materia Condensada,
Condensed Matter Physics Center (IFIMAC), and Instituto de Ciencia de Materiales Nicolás Cabrera,
Universidad Autónoma de Madrid, Madrid, 28049, Spain

Andrew O. Parry
Department of Mathematics, Imperial College London, London SW7 2BZ, UK

Carlos Rascón
GISC, Departamento de Matemáticas, Universidad Carlos III de Madrid, 28911 Leganés, Spain,

I. DENSITY DISTRIBUTION FOR A CORRUGATED SURFACE IN THE LANDAU-GINZBURG-WILSON APPROXIMATION

The non-local density distribution $\rho_\ell(x,z)$ shown in Fig. 1 of the main paper was calculated using a (dimension less) Landau-Ginzburg-Wilson (LGW) free-energy density functional

$$F[\rho(r)] = \int d^3\mathbf{r} \left(\phi\left(\rho(\mathbf{r})\right) + \frac{1}{2}\left(\nabla\rho(\mathbf{r})\right)^2 \right), \tag{1}$$

where the local free energy density ϕ is approximated by the asymmetric double parabola:

$$\phi(\rho) = \min\left(\frac{\kappa_l^2}{2}\left(\rho-\rho_l\right)^2,\ \frac{\kappa_v^2}{2}\left(\rho-\rho_v\right)^2 \right). \tag{2}$$

The bulk densities and corresponding inverse correlation lengths are taken from the simulation results for the LJ model. These are $\rho_l\sigma^3 = 0.805$, $\rho_v\sigma^3 = 0.01$, $\kappa_l\sigma = 1.5$ and $\kappa_v\sigma = 3.0$.

Minimization of (1) leads to the Euler-Lagrange equation

$$\nabla^2\rho(\mathbf{r}) = \begin{cases} \kappa_v^2\left(\rho(\mathbf{r})-\rho_v\right) & \text{for } \rho(\mathbf{r}) < \rho_m \\ \kappa_l^2\left(\rho(\mathbf{r})-\rho_l\right) & \text{for } \rho(\mathbf{r}) > \rho_m \end{cases} \tag{3}$$

where the matching density between the vapour and liquid phases is given by

$$\rho_m = \frac{\kappa_l\rho_l + \kappa_v\rho_v}{\kappa_l+\kappa_v}. \tag{4}$$

We define the interfacial shape $\ell(\mathbf{x})$ to be the surface of isodensity $\rho(\mathbf{r}) = \rho_m$, where $\mathbf{r} = (\mathbf{x}, \ell(\mathbf{x}))$. Assuming that the interfacial shape is $\ell(\mathbf{x}) = \ell_q\cos(q\ x)$, the solution to the PDE is

$$\rho(\mathbf{r}) = \begin{cases} \rho_v + \displaystyle\sum_{n=0} B_n e^{\beta_n z}\cos(n\ q\ x) & \text{for } z < \ell(\mathbf{x}) \\ \rho_l - \displaystyle\sum_{n=0} A_n e^{-\alpha_n z}\cos(n\ q\ x) & \text{for } z > \ell(\mathbf{x}) \end{cases} \tag{5}$$

where $\alpha_n = \sqrt{\kappa_l^2 + (n\ q)^2}$ and $\beta_n = \sqrt{\kappa_v^2 + (n\ q)^2}$. The coefficients A_0, A_1,..., B_0, B_1,..., are obtained by matching the densities at $z = \ell(x)$, which yields the two linear equations:

$$\sum_{n=0} A_n e^{-\alpha_n \ell(x)} \cos(n\ q\ x) = \kappa_v \frac{\rho_l - \rho_v}{\kappa_l + \kappa_v} \tag{6}$$

and

$$\sum_{n=0} B_n e^{\beta_n \ell(x)} \cos(n\ q\ x) = \kappa_l \frac{\rho_l - \rho_v}{\kappa_l + \kappa_v}. \tag{7}$$

For a planar interface, the derivatives also match.

The density $\rho(x, z)$ plotted in Fig. 1 of the main article is the numerical solution for $q\sigma = 2$ and $\ell_q = 0.1\sigma$. The matching equations were solved by series expansion of the exponentials up to order ℓ_q^4. Finally, we calculate the $\mathbf{x}$-averaged density profile $\rho_{\mathbf{x}}(z)$. With respect to the asymptotic decay into the bulk phases, this average mimics the thermal average of equation (5) in the main article, since it is equivalent to averaging over the set of harmonic interfacial fluctuations at fix q and ℓ_q.

II. GAUSSIAN FILTER

We use a Gaussian filter to improve the accuracy of our simulation results, which allows us to obtain the decay lengths for the equilibrium density profile $\rho(z)$ and for the Fourier transformed correlation function $\tilde{C}(q, z)$. The raw simulation results are filtered by convoluting with a Gaussian which, for the density profile, reads

$$\rho_{filtered}(z) = \frac{1}{\sqrt{2\pi\Delta}} \int \rho(z') \exp\left(-\frac{(z - z')^2}{2\Delta}\right) dz', \tag{8}$$

This effectively smoothes the data between neighboring histogram bins, which have a width of $\delta z = 0.125\sigma$. In Fig. 1, we plot the raw (blue empty circles) and filtered (full black circles) density profiles near the liquid-vapour interface. Although both density profiles decay exponentially towards the bulk in agreement with the theoretical prediction given by

$$\rho(z) - \rho_l \sim \exp(-\kappa z), \tag{9}$$

the filtering reduces the noise by a factor of 100. For $\Delta = 0.5\sigma$, we obtain our best estimate for $\kappa\sigma = 1.5 \pm 0.05$.

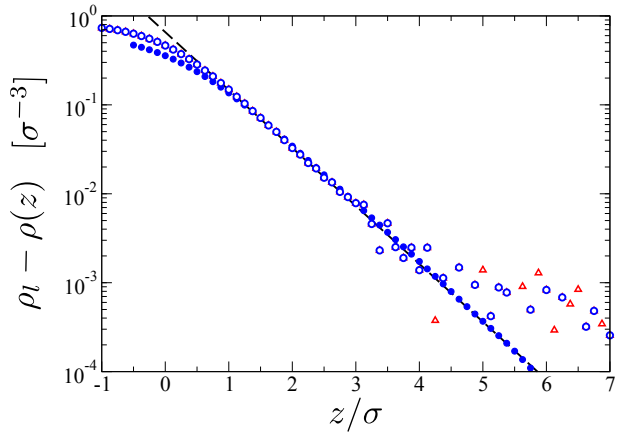

FIG. 1: (Color online) The empty circles show the raw equilibrium density profile $\rho_l - \rho(z)$. The red triangles also represent the raw data for $|\rho_l - \rho(z)|$ when $\rho_l - \rho(z) < 0$. The full circles are the filtered values using a Gaussian of width $\Delta = 0.5\sigma$. Note that the filtered results have been shifted to match the raw data, since filtering produces a function with the same exponential decay but slightly displaced. This figure corresponds to the inset of Fig. 2 in the main article.

For the correlation function $\tilde{C}(q, z)$, we use a similar filter as above:

$$\tilde{C}_{filtered}(q, z) = \frac{1}{\sqrt{2\pi\Delta}} \int \tilde{C}(q, z') \exp\left(-\frac{(z - z')^2}{2\Delta}\right) dz', \tag{10}$$

Figure 2 shows the results for $\tilde{C}(q,z)$, obtained using the ISM to define the interfacial position, for three values of $q\sigma = 0.15$, 0.90 and 1.29. The black empty circles correspond to the raw data for $q\sigma = 0.15$. We observe an exponential decay towards the bulk liquid

$$\tilde{C}(q,z) \sim e^{-\kappa_{\rm MD}(q)z}, \tag{11}$$

over a distance of $\approx 2\sigma$, until the signal goes below the noise $\sim \pm 0.0001$. In order to reduce the noise level, we use the Gaussian filter to gain a factor of 100 in the detected decaying signal. The stars in Figure 2 show the optimally filtered results, obtained by using different values of Δ over the range of z. In this way, we can identify the values of $\kappa_{\rm MD}(q)$, obtained from (at least) two decades in $\tilde{C}$, even for wavevectors $q\sigma > 1.0$. One can also see the ultimate asymptotic oscillatory decay of $\tilde{C}(q,z)$ for large z and q.

Finally, we comment that, in order to see non-local effects (that is, the q dependence of $\kappa_{\rm MD}$), it is necessary to consider wave vectors $q\sigma \approx 1$. In turn, this means that our definition of the interface shape $\ell(\mathbf{R})$ must remain 'good' down to wavelengths of a few molecular diameters. The (percolative) ISM does this, but other (simpler) definitions, for example the Local Gibbs Dividing Intrinsic Surface[? ? ?], which would work perfectly well in the (macroscopic) low$-q$ limit, fail completely in this respect[? ?].

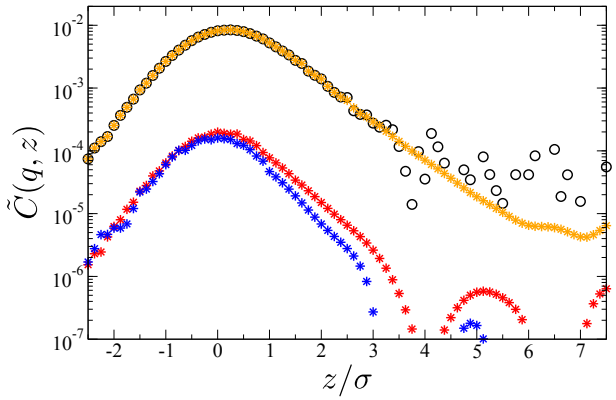

FIG. 2: (Color online) Correlation function $\tilde{C}(q,z)$ *vs.* z for different values of q: orange stars ($q\sigma = 0.15$), red stars ($q\sigma = 0.90$) and blue stars ($q\sigma = 1.29$). Also shown is the unfiltered data for $q\sigma = 0.15$ (circles). This figure corresponds to the inset of Fig. 3 in the main article.